TTK4550 SPECIALIZATION PROJECT

System Identification of an Unmanned Surface Vehicle With Fixed Dual Thrusters

Jenny Aurora Frøland Steindal

Fall 2018

Supervisor: Prof. Tor Arne Johansen
Co-supervisors: Stephanie Kemna (Maritime Robotics)

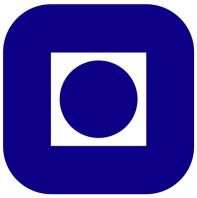

FACULTY OF INFORMATION TECHNOLOGY AND ELECTRICAL ENGINEERING
DEPARTMENT OF ENGINEERING CYBERNETICS
NORWEGIAN UNIVERSITY OF SCIENCE AND TECHNOLOGY

Abstract

Unmanned surface vehicles (USVs) have been around for over 70 years and have been important vessels in warfare, oceanography and industry. Maritime Robotics (MR) make several different USVs, including the Otter, which is used in the mapping of the seabed and monitoring, sheltered waters. The Otter is a USV with a fixed dual thruster setup. In this report I focus on how to obtain model parameters for the Nomoto model, which is the proposed autopilot for the Otter USV.

Before the model parameters can be obtained, a model describing the relation between force and rpm for the propellers has to be obtained. This is done by conducting a series of practical tests on the water with the Otter USV. First, the propeller parameter and torque is obtained by doing a bollard pull test, followed by performing turning circles, where the input (rpm for both propellers) and the output (turning rate) are logged. These experimental data are then used to obtain the model parameters by nonlinear least square curve fitting.

Here, I show that the experimental data indicate asymmetry when the unmanned surface vehicle (USV) turns to port and starboard. This can be explained by the fact that both the propellers are rotating clockwise when moving forward meaning that the USV will rotate to port due to conservation of angular momentum. Moreover, the torque produced by the propellers is presented as the input to the Nomoto model. The bollard pull test indicated that the thrusters are saturated when hitting 80% and above. When performing a turning circle using the thrusters in opposite direction the turning is far less effective due to the propeller's asymmetric design. Two models were made; one for fast turning and one for slow turning. To compensate for the extra torque to port side, two correction terms depending on each thruster are added to the original input torque.

Contents

Nomenclature

δ	Rudder angle
ω_i	Rotational speed of the propellers
ψ	Yaw, heading
a	Moment arm for each thruster
F_i	Thrust from each propeller
K	Nomoto gain (system parameter)
Q_p	Applied torque from the thrusters. Input torque for the Nomoto model
r	Yaw rate
T	Nomoto time constant (system parameter)
T_p	The total thrust for the USV. Input to a surge speed model
u	Surge speed
IMU	Inertial measurement unit
RPM	Rotations per minute
USV	Unmanned surface vehicle

Chapter 1

Introduction

1.1 Background

An unmanned surface vehicle (USV) is a vehicle which operates with close to continuous contact with the water surface, has been used since the Second world war (Breivik, 2010). At that time, the USV was a small radio controlled boat, which performed dangerous missions, e.g. as a tool in mine sweeping operations, or as shooting targets for manned marine vessels.

After World War II, the focus shifted towards developing advanced unmanned vehicles operating in the air or under the water surface. As a consequence, developing the USV was not a priority. However, in the beginning of the 1990s it was established an interest of developing advanced technology for the USV. Monotone tasks such as seafloor mapping is an application for the USV. This will reduce cost and reduce the security risk for the crew.

The Otter is an unmanned surface vehicle developed by Maritime Robotics. Maritime Robotics was founded in 2005, they make vehicle control systems and sensors for Unmanned vehicles. The Otter USV has a catamaran hull, measuring $200 \times 105 \times 85$ millimetres, and is the smallest USV produced by Maritime Robotics and is used in seabed mapping and monitoring of sheltered waters. The Otter USV is equipped with two fixed propellers, which means that turning the vessel is executed by the different forces form the propellers. In this paper, I will present a possible autopilot model for the Otter, as well as how to obtain the system parameters. A thrust allocation is also made, in order to make an input corresponding to the proposed model.

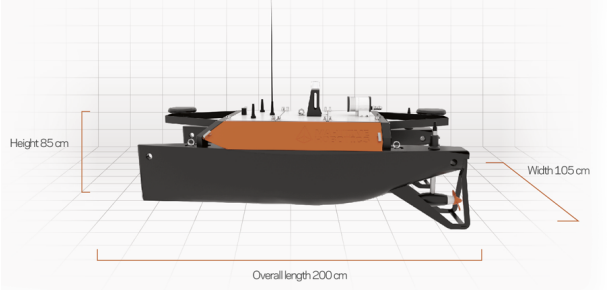

Figure 1.1: Otter USV. Courtesy to Maritime Robotics

Problem description

The main task in this paper is to obtain a system model for the Otter USV and find the model parameters. Figure 1.2 summarise the interaction between all the sub-tasks completed in this paper. The numbers denote the order the sub tasks were completed and are presented in detail in Chapter 2.

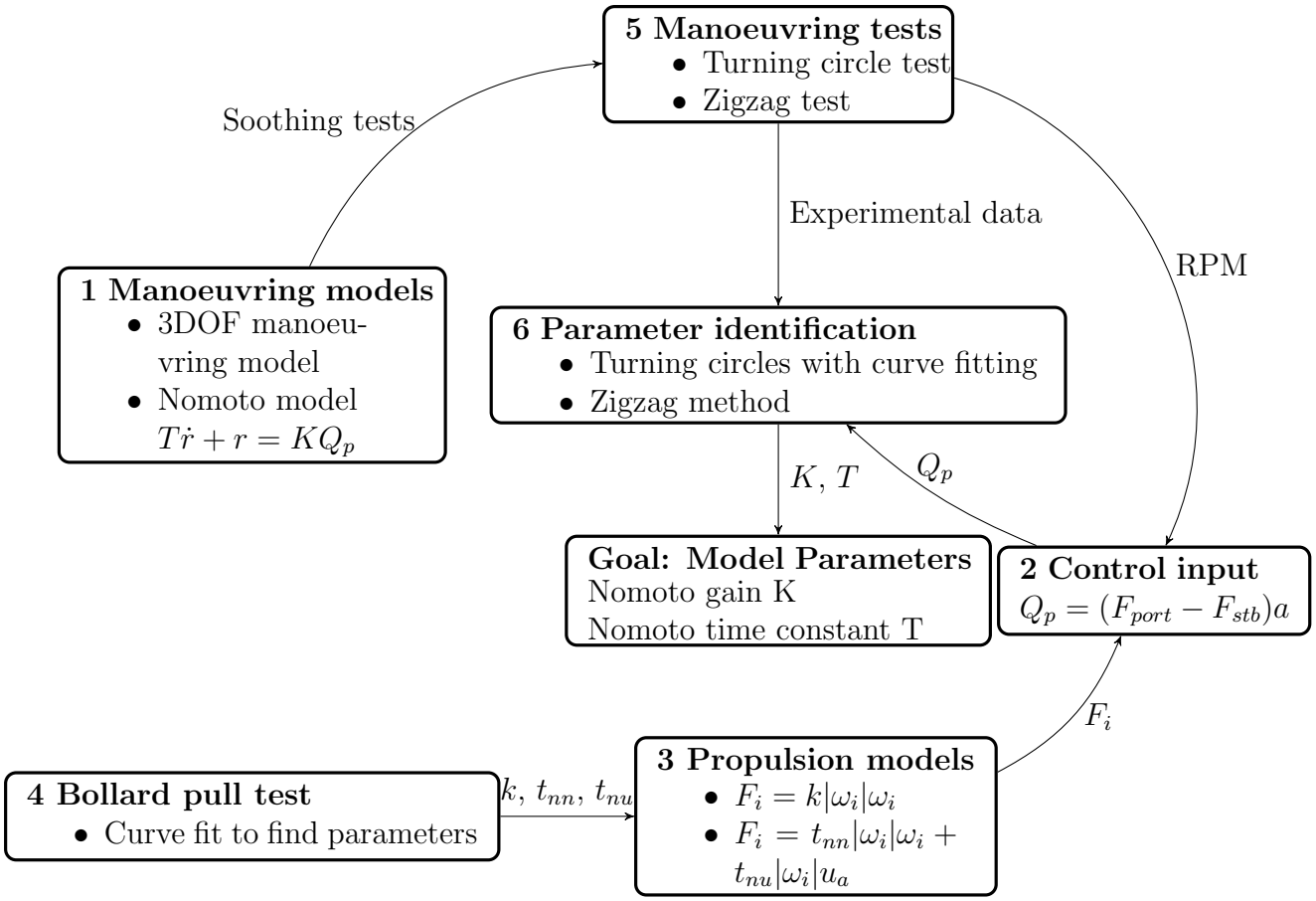

Figure 1.2: Description of the all the elements in the paper and how they interact

Objectives

- State a system model for the Otter USV
- Live testing to determine system parameters (system identification)
- Thrust allocation to compute the general control forces in terms of control inputs from the fixed propellers

Limitations

Due to lack of time the manoeuvring tests was done only once. Furthermore, the weather conditions for the tests were sub-optimal which means the data obtained and used in the model is not as accurate as they could have been.

1.2 Outline

Chapter 2

This chapter describes the theory behind the proposed model, manoeuvring tests, identification methods and thrust allocation. It also describes how the inputs are defined and proposes propulsion models for the thrusters.

Chapter 3

This chapter describes how the bollard pull and manoeuvring tests were done. This chapter also contain a code snippet of how the model parameters were obtained.

Chapter 4

This chapter presents the results and discuss possible explanations for the obtained results.

Chapter 2

Theory

2.1 System Identification

The core of system identification is to make a mathematical model based on experimental evidence. Figure 2.1 shows the flow of the system identification procedure. Input and output signals from experimental tests are logged, and subsequent data analysis is performed in order to construct a model (Ljung, 1998). The most important step of system identification is perhaps to choose the right model structure. When there is no prior knowledge of the system's internal structure, the model is chosen without reference to the physical background. This is called black-box modelling. In contrast, when there is prior knowledge of the system's structure which can be combined with data, it is called grey-box modelling.

The steering dynamics of boats is nothing new, which means there is a lot of knowledge about the internal structure of boats present. Based on this knowledge, the system identification performed in this report follows grey-box modelling. When choosing a model structure, a simple model is a good way to start. The manoeuvring model proposed for the Otter USV is a first order linear differential equation proposed by Nomoto et al. (1957) and served as a natural place to start. This report will therefore investigate if the first order Nomoto model is a good fit for describing the Otter USV's manoeuvring.

The first order Nomoto model has two model parameters. In order to identify these two parameters, different manoeuvring tests have to be performed. These tests will generate experimental data for input and output which will be used by a nonlinear least square curve fitting algorithm.

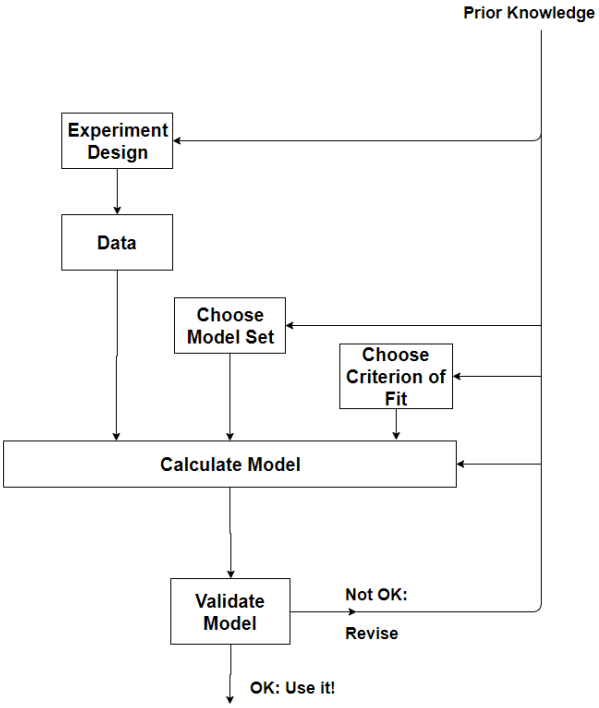

Figure 2.1: System identification loop from Ljung (1998)

2.2 The Otter USV

The Otter USV moves in six degrees of freedom (DOFs). To determine the position and orientation, six independent coordinates are necessary which is depicted in figure 2.2. The horizontal movement of a ship can be described by a 3 DOF manoeuvring model. Where the motion component surge, sway and yaw describe the horizontal movements. This implies that pitch, heave and roll are equal to zero, which mean they are neglected in the 3 DOF manoeuvring model (Fossen, 2011).

When a vessel is moving at slow varying forward speed, the 3 DOF manoeuvring model can be decoupled into two subsystems; surge speed subsystem and sway-yaw subsystem. The sway-yaw subsystem is used when deriving the 1 DOF manoeuvring model, known as the Nomoto model. This model expresses the dynamics of the yaw rate, i.e. the rate of turn around the z_b axis, which is depicted in figure 2.3

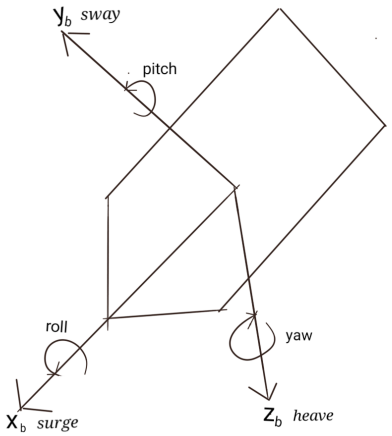

Figure 2.2: The Otter USV's 6 DOF

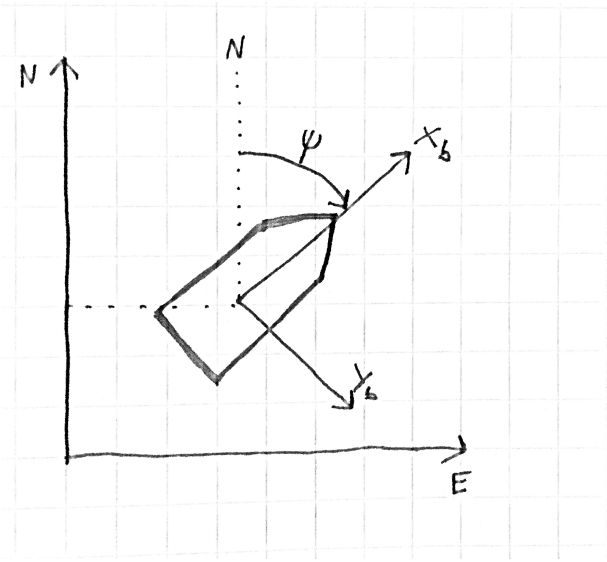

Figure 2.3: The planar motion with defined yaw angle

2.3 Autopilot Model

For an unmanned surface vehicle, an autopilot model is a preferable tool to obtain knowledge of the steering qualities of a vessel. The autopilot model can be used to obtain an autopilot, which means the vehicle can be controlled without constant human intervention. An autopilot model gives valuable information about a vessel's heading dynamics which can be used when designing an autopilot. In theory if the model is good enough, the USV can be controlled just through feed forward. However, due to waves and other disturbances, feedback control is necessary in reality. The autopilot model can also contribute

with information about the heading if the sensor system is down.

2.3.1 The Nomoto Model

Several different autopilot models exists for marine crafts. A widely used model for heading controller for ships is the proposed model by Nomoto et al. (1957), which is also the model proposed for the Otter USV. The Nomoto model is preferred over other autopilot models as it has an easy structure and describes the heading dynamics as a linear system.

The second-order Nomoto model can be derived from the linearized 2 DOF manoeuvring model (sway-yaw subsystem) (Fossen, 2011). The model can be written as

$$\mathbf{M}\dot{\boldsymbol{\nu}} + \mathbf{N}(u_0)\boldsymbol{\nu} = \mathbf{b}\delta \tag{2.1}$$

where δ is the rudder angle and $\boldsymbol{\nu} = [v, r]^\top$ where v is the sway velocity and r is the yaw rate. This model is based on the assumptions that v and r are small and that the cruise speed u is approximately constant.

$$u = u_0 \approx \text{constant} \tag{2.2}$$

Choosing r as the output

$$r = \begin{bmatrix} 0 & 1 \end{bmatrix} \boldsymbol{\nu} \tag{2.3}$$

Thus, applying the Laplace transform, the second order Nomoto model yields

$$\frac{r}{\delta}(s) = \frac{K(1 + T_3 s)}{(1 + T_1 s)(1 + T_2 s)} \tag{2.4}$$

To obtain the first-order Nomoto model a new time constant is defined as

$$T := T_1 + T_2 - T_3 \tag{2.5}$$

the first order Nomoto model becomes

$$\frac{r}{\delta}(s) = \frac{K}{(Ts + 1)} \tag{2.6}$$

Using $\dot{\psi} = r$ the obtained result for a heading autopilot model is

$$\frac{\psi}{\delta} = \frac{K}{s(Ts+1)} \tag{2.7}$$

Nomoto (1960) explained the parameter K as the vessel's turning ability. The larger the K value of a ship, the greater the turning angular rate, r, and subsequently a smaller steady turning circle.

T is explained as the vessel's course-stability and quick response in steering. The quickness of a vessel to approach the terminal angular rate is determined by T. The smaller the T, the quicker buildup of the turning angular rate. This can be seen in equation (2.16).

2.4 Control Inputs

The Otter USV is an underactuated vessel. This means that the USV is moving in more degrees of freedom than it has control inputs (Fossen, 2011). For the 3 DOF manoeuvring model it is sufficient to have one control input in yaw and one control input in surge to steer the USV along a path.

Up until now, the input of the Nomoto model is described with a rudder angle, δ. When a rudder angle is given, the boat starts to turn due to the applied torque from the rudder. However, the Otter USV does not have a rudder, but is equipped with two fixed propellers which steers the vessel. To make the Otter USV turn, a difference in thrust is used ($F_{port} \neq F_{starboard}$) to create a torque. If the difference in thrust is multiplied with the moment arm, a, depicted in figure 2.5, the torque is obtained. The positive torque is found using the right hand rule, the z_b-axis are pointing downwards, as depicted in figure 2.2. This means that a starboard turn gives positive torque. Moreover, the input to the Nomoto model is torque. The torque given to the Otter USV can be defined as

$$\begin{aligned} u_1 &= Q_p = (F_{port} - F_{stb})a \quad [\text{Nm}] \\ u_2 &= T_p = F_{port} + F_{stb} \quad [\text{N}] \end{aligned} \tag{2.8}$$

where Q_p is the propeller torque and T_p is the total thrust. F is the thrust from each propeller. The moment arm, a, is depicted in figure 2.5. Input u_2 can be used as input to a surge model.

The block diagram depicted in figure 2.4 shows the relation from propeller shaft speed, ω_i, to the control input, u_1.

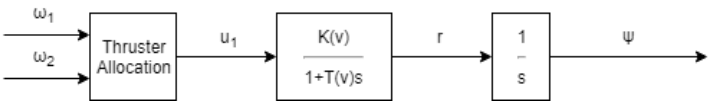

Figure 2.4: Block diagram of the system

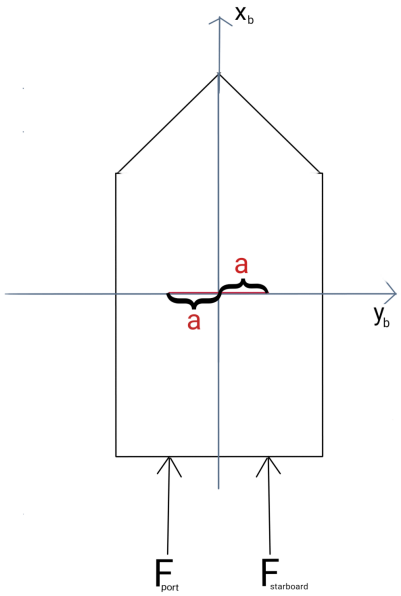

Figure 2.5: Control forces for the USV and the moment arm

2.5 Thrust Allocation

The thrusts, F_i, introduced in section 2.4 have to be found. The generalised control forces acting on the Otter USV are depicted in figure 2.5. The purpose of thrust allocation is to deliver the generalised control forces to the thrusters in terms of control inputs, which are rotations per minute (RPM) for the Otter USV. (Fossen, 2011).

2.5.1 Propulsion Models

In order to calculate the control forces generated by the propellers, a model for the propellers have to be obtained.

A model structure for the propellers is found in Blanke et al. (2007). This model takes into account the moving speed of the vessel and the propeller rpm. The model is described

the following way:

$$F_i = t_{nn}\omega_i|\omega_i| + t_{nu}|\omega_i|u_a \tag{2.9}$$

where ω is the propeller shaft speed, t_{nn} and t_{nu} are propeller parameters. u_a is the advance speed given by

$$u_a = U_a + u_w \tag{2.10}$$

where U_a is the nominal advance speed and u_w is the induced water speed.

$$U_a = (1 - w_f)u \tag{2.11}$$

where u is the vessel speed and w_f is the wake fraction

Another thruster model is

$$F_i = k\omega_i|\omega_i| \tag{2.12}$$

This model only considers the square term, and is not dependent on the vessel's speed. The parameters of the proposed propulsion models (2.9) and (2.12) are identified by performing a bollard pull test, described in section 2.6.

Symbol	Description	Unit
t_{nn}, t_{nu}, k	Propeller parameters	-
u_a	Advance speed	m/s
U_a	Nominal advanced speed	m/s
ω	Propeller shaft speed	rad/s
w_f	Wave fraction	-
u_w	Induced water speed	-

2.6 Bollard Pull Test

A bollard pull test is used to determine a marine vessel's pulling power (Jukola and Skogman, 2002). The vessel is towed to a bollard, so that when the vessel is pulling on the towline, it is exerting a force which is measured by a scale. At the same time the RPM from the thrusters are read.

The bollard pull is a product of propeller thrust and the interaction between the hull of the vessel and the propellers. By performing a bollard pull test the propeller parameter

for (2.12) can be obtained. These parameters describe the relationship between the thrust and the control input (RPM).

The bollard pull test can also be performed for different advance speed to obtain the propeller parameters to thruster model (2.9). The advance speed can be obtained by using a tow carriage as described in Li and Bachmayer (2013).

The trial site has a large impact on the the bollard pull, and some conditions has to be considered when choosing the trial site. The conditions for a bollard pull test are retrieved from Jukola and Skogman (2002) and is explained in the section below.

2.6.1 Trial Site

The optimal location for the bollard is to be located on a legged jetty with no walls, such that the propeller wake will flow under the jetty. If the bollard is located on a solid pier, it should be placed such that the propeller wake has a clear run.

Water Depth

To avoid a build up of circulation, the water depth should be as large as possible. The required minimum depth can be calculated using the formula:

$$d_{min} = 0.060 \cdot (52.0 \cdot P^{0.60} - 46.26 \cdot P^{0.61}) + 3 \quad [\text{m}] \tag{2.13}$$

where P is the total propulsion power [kW].

Rope Length

In general the rope length should be as long as possible. This is to avoid circulation due to the propellers. The minimum rope length should not be less than the following equation:

$$L_{min} = 52.0 \cdot P^{0.60} - 46.26 \cdot P^{0.61} \tag{2.14}$$

2.6.2 Environmental Conditions

Wind Speed

During the trials the wind speed should not exceed 5 m/s

Current

The test should be done in waters with no current. If current is present it should not exceed 1 knot.

If the test area has tidal current, the recommended procedure is to perform the test 1.5 hours before high tide. This is because the current speed is low and the water level is close its maximum.

2.7 Manoeuvring Tests

The Nomoto parameters as described in section 2.3.1 can be obtained through performing manoeuvring tests. The proposed manoeuvring tests are comprised of a zigzag test and a turning circle and will be described in the sections below.The input and output data acquired from these two tests can in turn be used to identify the Nomoto parameters. When making a model based on experimental data, the data should not be affected by environmental disturbances. This is to avoid disturbances affecting the finished model. Since the disturbances varies over time and location it is not an advantage to include in the model. However, it should be handled by the controller.

The zigzag test consists of several steps, and yields input data which contains information about the dynamics of the system which can be used to identify the Nomoto parameters, K and T. This is described in section 2.8.2. However, when the vessel performs a circle in the turning circle test the yaw rate will, after some time, be constant. This can be used to identify the model parameters based on solving the first order differential equation describing the Nomoto model. By using a nonlinear curve fit method, the solved equation can be used to obtain the Nomoto parameters. This is described in section 2.8.1.

2.7.1 Kempf's Zigzag Test

The zigzag test is performed by measuring the heading angle, ψ, while the vessel gets a step input which results in the vessel changing the heading angle. When the heading angle is measured to 10° the opposite step is given as an input. This is described in the figure below. After 5 input steps are executed the test is done.(Gertler and Gover, 1960)

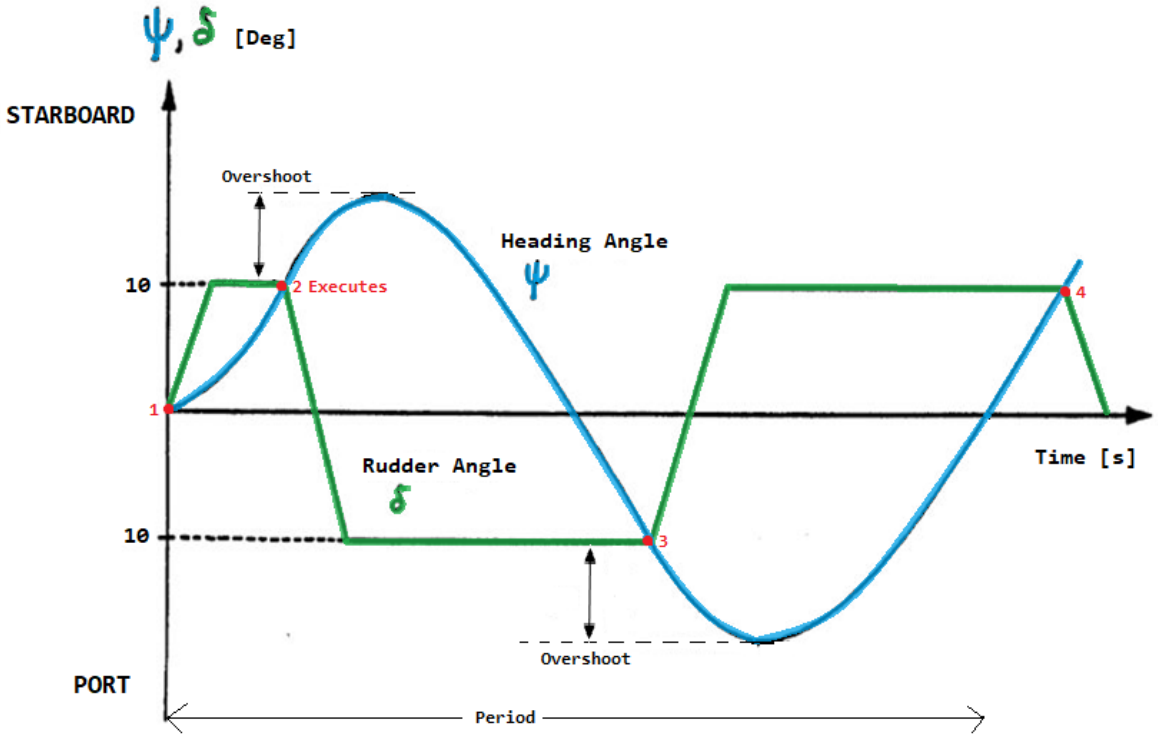

Figure 2.6: Zigzag manoeuvre (Gertler and Gover, 1960)

2.7.2 Turning Circle

A turning circle is performed by applying a constant rudder angle driving the vessel to turn in a circle. According to the International Towing Tank Conference (ITTC, 2002), a turning circle trial should be performed the following way: At first, the vessel has a constant speed. This can be seen in figure 2.7 as the straight line. Second, the maximum rudder angle is applied and the vessel starts to turn. The vessel should perform a 540° turn to be able to identify all the parameters of this test. The parameters that can be identified from this test are:

- Tactical turning diameter
- Steady turning diameter
- Advance
- Transfer
- Time to change heading to 90° and 180°
- Loss of speed on steady turn

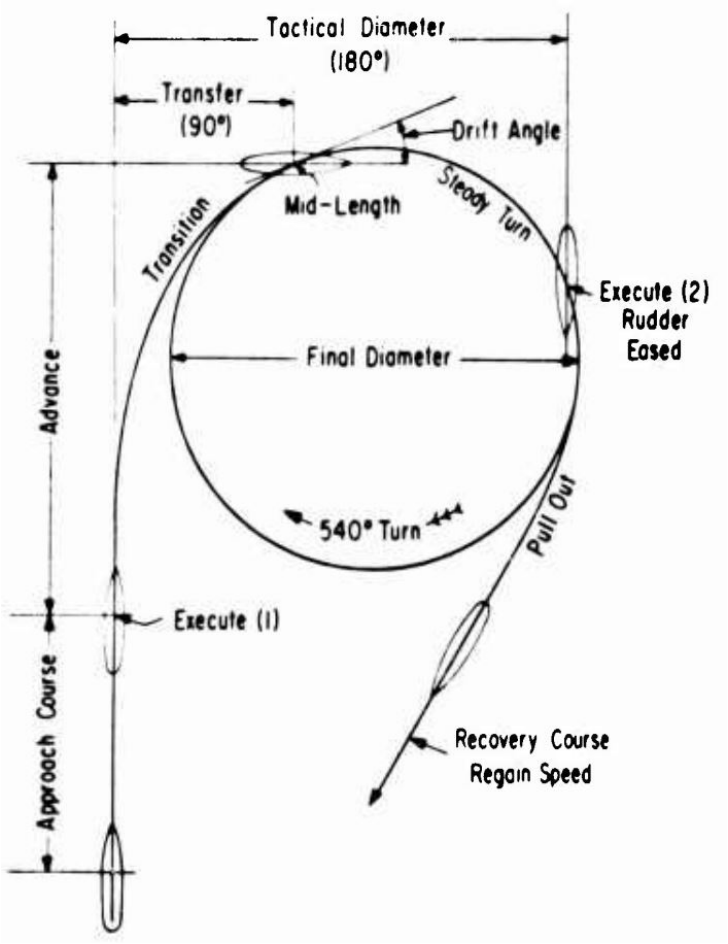

Figure 2.7: Turning circle trial (Gertler and Gover, 1960)

2.8 Identification Methods

2.8.1 Parameter Estimation Using Least Square Fitting

A proposed solution on how to find the model parameters, K and T, can be found in Fossen (2011). To find the parameters of the Nomoto model the torque, Q_p, and the yaw rate, r, need to be logged. These experimental data can be obtained by performing a turning circle. The inverse Laplace transform of the equation (2.6) the steering motion of a ship in time domain can be described as

$$T\dot{r} + r = KQ_p \tag{2.15}$$

The next step is to solve the differential equation (2.15) to obtain:

$$r(t) = e^{-\frac{t}{T}}r(0) + (1 - e^{-\frac{t}{T}})KQ_p \tag{2.16}$$

Using nonlinear least square curve fitting to (2.16) the parameters of the Nomoto model can be estimated.

2.8.2 Parameter Estimation Using Kempf's Zigzag Test

This procedure is another way of estimating the parameters of the Nomoto model. After performing the zigzag test described in section 2.7.1, the Nomoto parameters can be identified using the following method: Moreira et al. (2005) describes the procedure and in figure 2.8 the integral term is shaded. The shaded areas and the marked data points are used in (2.20) and (2.21) to calculate the model parameters.

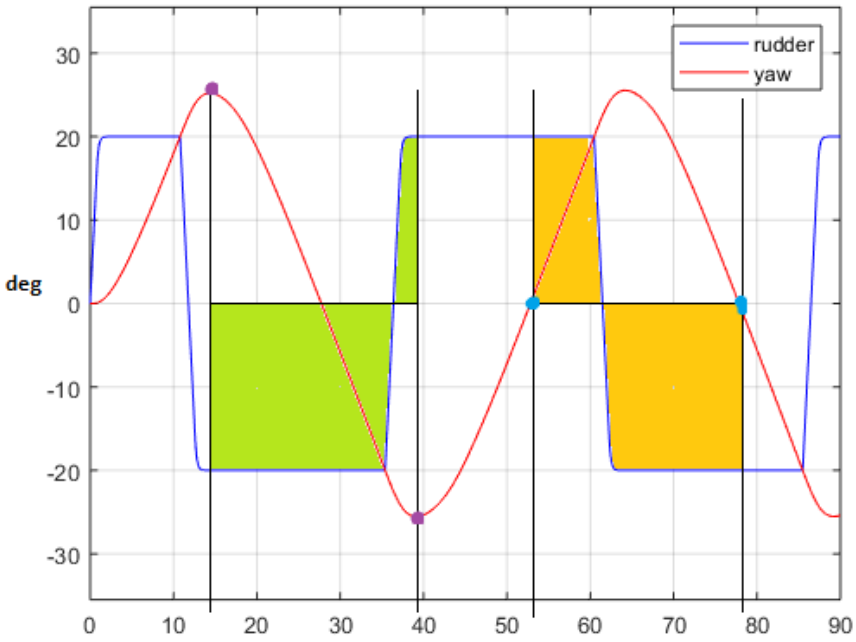

Figure 2.8: Notation for the zigzag manoeuvre. Courtesy of (Moreira et al., 2005)

The Nomoto parameters can be calculated the following way

$$T\dot{r} + r = K\delta \tag{2.17}$$

Integrating (2.17) with respect to time:

$$T\int_0^t \dot{r}dt + \int_0^t rdt = K\int_0^t \delta dt \tag{2.18}$$

The left hand side can be expressed as

$$T\left[r\right]_0^t + \left[\psi\right]_0^t = K\int_0^t \delta dt \tag{2.19}$$

$$K = -\frac{\psi_1 - \psi_2}{\int_{t_1}^{t_2} \delta(t)dt} \tag{2.20}$$

where the green shaded area in figure 2.8 is the integral term from t_1 to t_2. The purple dots mark ψ_1 and ψ_2.

$$\frac{K}{T} = -\frac{r_4 - r_3}{\int_{t_3}^{t_4} \delta(t)dt} \tag{2.21}$$

When the heading (ψ) is crossing zero degrees the yaw rate (r) is read, these are marked with blue dots. The yellow area marks the integral term from t_3 to t_4

However there are other methods to obtain the Nomoto parameters from the zigzag test. These are described by Golikov et al. (2018), Azarsina and Williams (2012), Journée (1970)

Chapter 3

Method

3.1 Bollard Pull Test

The bollard pull test was conducted by the pier close to Maritime Robotics's office in Trondheim, Norway, on November 19, 2018, between 11:15 and 11:36. It was clear weather with a mean temperature of -2° Celsius and no wind. During the test period the tide was decaying with 12 cm. Kartverket (2018). However, Trondheim harbour is not known for strong tidal current, so therefore we assumed no current in the trial cite.

3.1.1 Equipment

- Asaklitt compact digital luggage scale, capacity 50 kg
- Rope
- Otter USV
- Computer to give thruster commands

3.1.2 Setup

The measurements were conducted using a digital luggage scale. The scale was tied to a bollard at the dock and the Otter as shown in figure 3.1. The thruster values were set from 10 to 100 % of maximum throttle, with interval of 10. The rpm was logged with a sampling rate of 2 Hz. The length of the rope from the scale to the Otter was 6 meter, which is sufficient to avoid circulation.

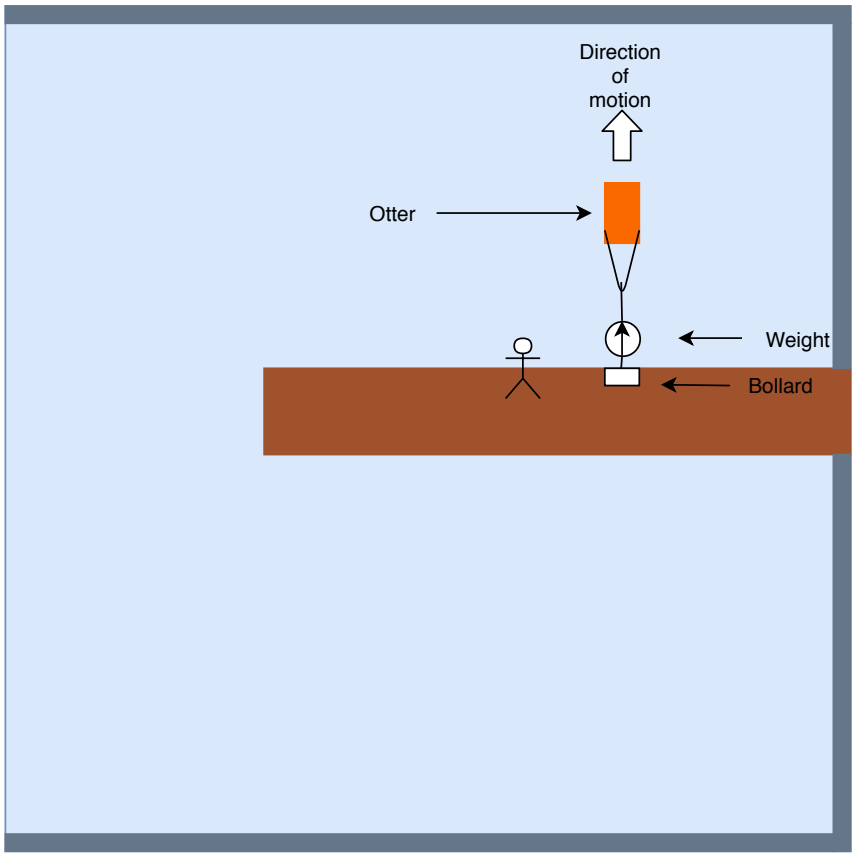

Figure 3.1: Illustration of the test environment.

The code uses curve fit to find the propeller parameters based on the model structure.

```
% Mean of both thrusters in rad/s
propeller = [0 122.4 243.7 358.8 490.5 615.8 725.6 844.6 981.4 980.6 980.9]'*pi/30;

% Measured thrust
thrust = [0 0.8 1.3 2.9 5.4 8.7 12.2 17.7 23.3 23.1 23.7]'*9.81;

%% Nonlinear Least Squares
% Model: ax^2+bx
 % Specify fit method
s = fitoptions('Method','NonlinearLeastSquares',...
               'Lower',[0,0],...
               'Upper',[inf,max(propeller)],...
               'Startpoint',[0 0]);

f1 = fittype('a*x^n+b*x','problem','n','options',s);
                                        % Model structure

[curve_fit,gof] = fit(propellers,thrust,f1,'problem',2);
                                    % Fit of object and goodness of fit
```

3.2 Manoeuvring Tests

The original plan was to execute both turning circles and zigzag manoeuvres. However, as there was no access to the compass during testing, the zigzag test could not be performed. Due to time limitations, a decision was made to exclude the zigzag test.

Turning Circle

The manoeuvring tests were conducted just outside of Trondheim harbour, Norway, on November 21, 2018, between 12:30 and 15:00. The weather was clear and no wind. The mean temperature during the test period was 0.7° Celsius. However, small waves were present and some places a small current was measured.

3.2.1 Equipment

- Otter USV
- Computer to give thruster commands
- Inertial measurement unit (IMU)

3.2.2 Setup

The Otter USV was mounted with the frame backwards (a mistake), and a 25 kilo weight plate compensating for the absence of the sonar. Each sensor was logged with a sampling rate of 5Hz. The commanded thruster values were set in percentage. There are two different ways of turning the Otter USV. The turning circles are performed to port and starboard. Depicted in figure 3.2a, the opposing circle has the general control forces from the propellers acting in opposite direction. On the other hand, shown in figure 3.2b, the additive circle has the general control forces from the propellers acting the same way, however, one of the forces is less than the other, giving the USV a torque. The complete test plan is shown in table 3.1

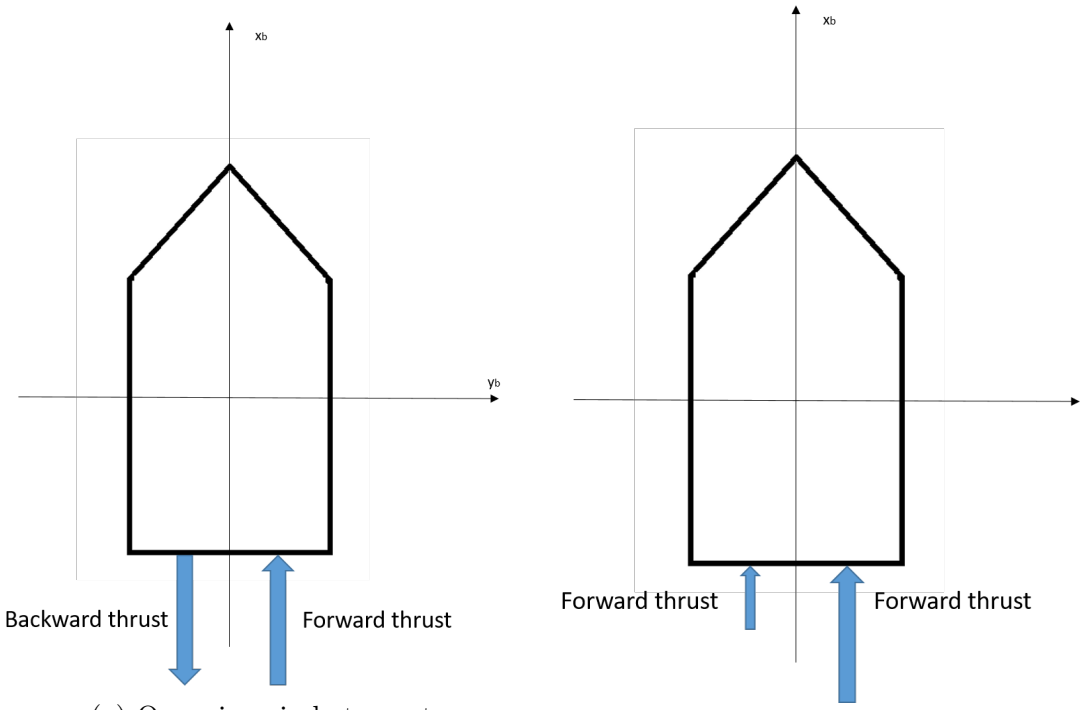

(a) Opposing circle to port

(b) Additive circle to port

Figure 3.2

	Additive		Opposing	
	Port turn	Starboard turn	Port turn	Starboard turn
Port thruster	10	100	-40	40
Starboard thruster	100	10	40	-40
Port thruster	15	60	-90	90
Starboard thruster	60	15	90	-90

Table 3.1: Test plan

3.3 Identification of the Nomoto Parameters

The used method to identify the Nomoto parameters is explained in section 2.8. In order to identify the coefficient x the `lsqcurvefit` function in MATLAB can be used. It tries to minimize equation (3.1) and obtain the coefficient x accordingly

$$\min_x ||\mathbf{F}(x, udata) - ydata||_2^2 = \min_x \sum_i (\mathbf{F}(x, udata_i) - ydata_i)^2 \tag{3.1}$$

were *udata* and *ydata* are input and output vectors respectively. $\mathbf{F}(x, udata)$ is a vector valued function which is user defined.(Mathworks, 2018)

$$\mathbf{F}(x, udata) = \begin{bmatrix} F(x, udata(1)) \\ F(x, udata(2)) \\ \vdots \\ F(x, udata(k)) \end{bmatrix} \tag{3.2}$$

The code used to obtain the Nomoto parameters, K and T, is described below.

```
load data.csv
%% Opposing 90 to starboard
starting = 59987;                       % Test starting
ending = 60431;                         % Test ending
yaw_rate = data(starting:ending,7);     % Yaw rate
thr_stb = -data(starting:ending,12);    % RPM from starboard propeller
thr_port = data(starting:ending,13);    % RPM from port propeller
k = 0.0002373;                          % Propeller parameter [N/rpm^2]
F_stb = k.*thr_stb.*abs(thr_stb);       % Force from starboard propeller
F_port = k.*thr_port.*abs(thr_port);    % Force from port propeller
a = 0.395;                              % Moment arm
M = (F_port-F_stb)*a;                   % Torque (input)

%% Nonlinear Curve Fitting
y = yaw_rate;                           % Output
N = ending-starting+1;                  % Samples
f = 5;                                  % Hz
time = (0:0.2:((N-1)/f))';

x0 = [0.1  1]';                         % Initial guess

F = @(x,time)(exp(-time*x(1))*0 + ...
x(2)*(1-exp(-time*x(1))).*M);           % Solved Nomoto equation

x = lsqcurvefit(F,x0, time, y);         % Nonlinear least square curve fit

T = 1/x(1)                              % Nomoto time constant
K = x(2)                                % Nomoto gain
```

Chapter 4

Results

4.1 Bollard Pull Test

Each thruster's rpm was logged with a sampling rate of 2 Hz. Moreover, the mean value of each thruster was calculated and is displayed in table 4.1.

Percentage thrust	Starboard thruster [rpm]	Port thruster [rpm]	Measured [kg]
10	123	122	0.8
20	243	244	1.3
30	359	359	2.9
40	490	491	5.4
50	615	617	8.7
60	726	725	12.2
70	844	845	17.7
80	984	979	23.3
90	980	981	23.1
100	984	977	23.7

Table 4.1: The results from the bollard pull test

Furthermore, the table shows the asymmetry between the thrusters. The differences are, however, rather small. An appropriate assumption is to take the mean of the two thruster's rpm and use it as input when estimating the propeller parameters. It is however worth to remark that according to this test, the thrusters seems to hit saturation at 80% of maximum throttle.

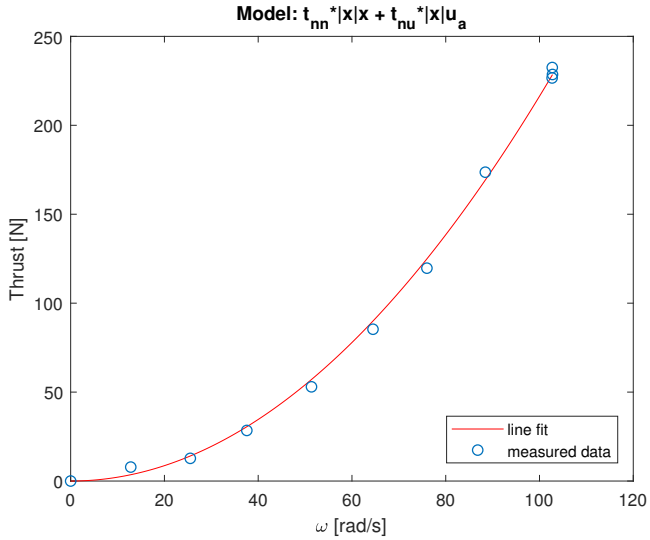

(a)

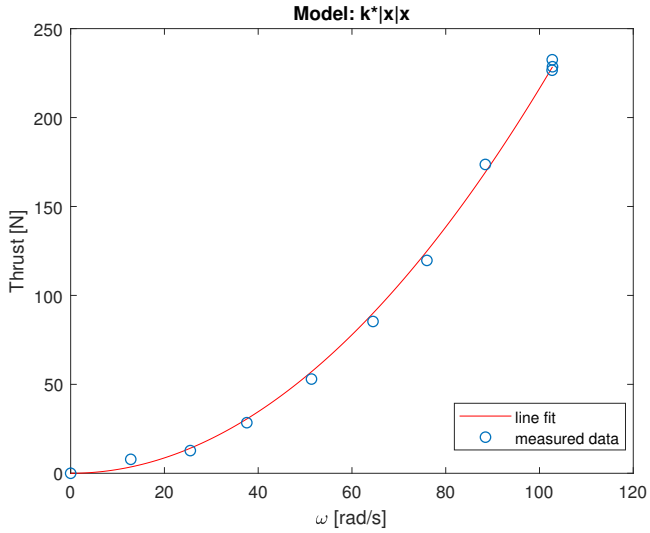

(b)

Figure 4.1: Curve fit was used to obtain the model parameters for each thruster model

In figure 4.1 the two models proposed in section 2.5.1 are fitted to the samples from the bollard pull test. The reason rad/s was the chosen unit is to have consistency with speed which is measured in m/s in (2.9). The estimated parameters of the two models are presented in table 4.2. However, since the bollard pull only was measured from a dock, the advance speed was 0. In this case, the two thruster models are equal, explaining the very low value of t_{nu}.

Model	Parameter square term	Parameter linear term
$F_i = k\omega_i\|\omega_i\|$	0.02164	-
$F_i = t_{nn}\omega_i\|\omega_i\| + t_{nu}\|\omega_i\|u_a$	0.02164	$5.653 \cdot 10^{-14}$

Table 4.2

When the advance speed is zero, the model $F_i = k\omega_i|\omega_i|$ is a good fit for the Otter USV's thrusters.

4.2 System Identification Results

Based on test setup presented in table 3.1, the following results were obtained for the turning circles:

The turning circles were divided into two categories; fast and slow turning. This is because the USV's dynamics are depending on the velocity. The fast turning consists of the tests opposing ±90 and additive 100/10. Slow turning consists of opposing ±40 and additive 60/15.

For both fast and slow turning, the measured yaw rate for all turning circles are noisy (green line in figure 4.2-4.5). However, the curve fitting manage to find the mean value of the measurements, and the static result is quite accurate. The estimated model responses acts like a low pass filter. However, looking at the time constant "T" for all turning circles the results is rather uncertain. The dynamics of the system is difficult to obtain, given just a simple step.

Comparing the estimated 1st order Nomoto model's response to port and starboard for all the different turning circles, the absolute value of the yaw rate is larger when the Otter USV are turning towards port. This happens regardless of velocity. To circumvent this problem, the measured yaw rate was tried filtered, using a moving average filter, but the filtered response did not contribute with any useful effect. The static results were not affected. The dynamics were clearer, however, due to measurement errors in the beginning, the dynamics are still inconclusive.

The input vector was made by obtaining the thrust for both propellers, using the rpm as input to the thruster model (2.12). The torque was calculated using (2.8) and the input vector was achieved and used in the curve fitting. This is shown in the code snippet in section 3.3.

Fast Turning

In figure 4.3, the opposing circle of ±90, the highest turning rate is measured. The high turning rate is expected due to large thrust acting in opposite direction. However, the difference between the additive and opposing turning rate are only approximately 1.3 deg/sec for a starboard turn. This can be due to the propeller design, which is designed asymmetric and the effect is decreasing significantly when rotating backwards.

The cruising speed of the USV was 2.45 m/s, and if the USV's thrusters depend on the advance speed, the thrusts can in fact have been reduced, contributing to lower turning rate.

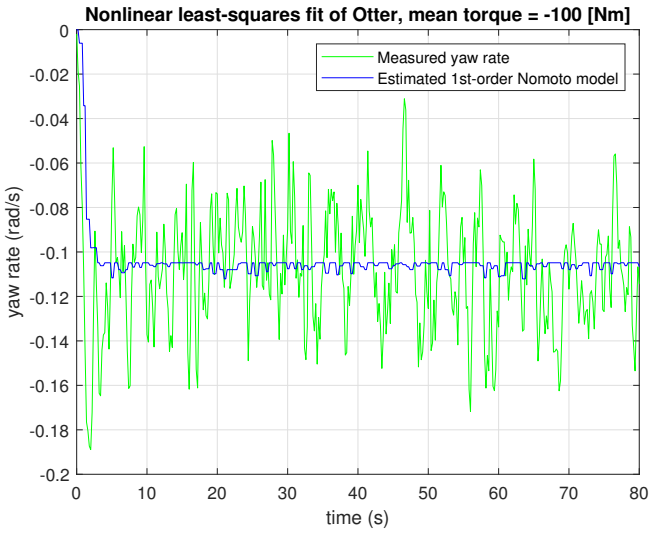

(a) Fast additive circle to port with input 100/10

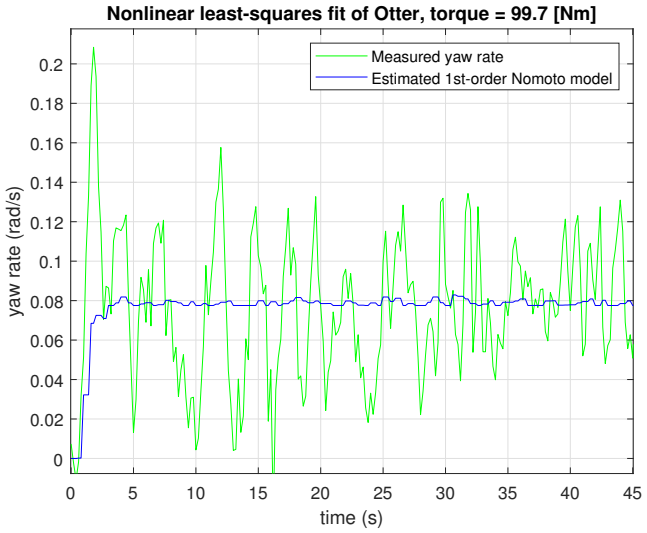

(b) Fast additive circle to starboard with input 100/10

Figure 4.2

Additive circle 100/10		
	Model parameters (Port)	Model parameters (Starboard)
K	0.0011	$7.8715 \cdot 10^{-4}$
T	0.4024	0.5076

Table 4.3: Identified model parameters for fast additive circle

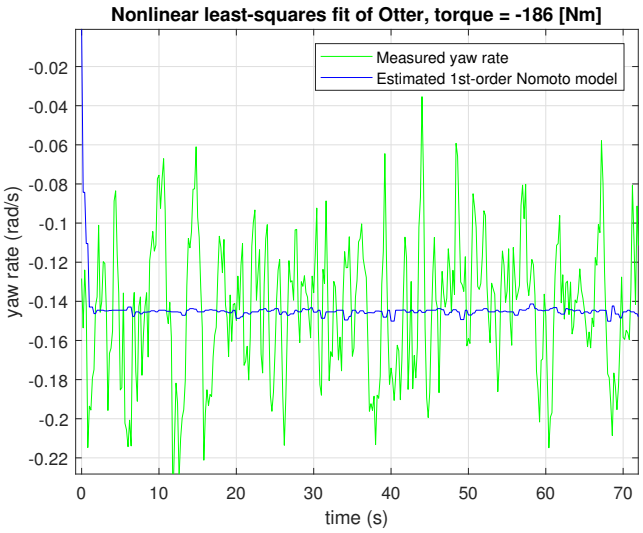

(a) Opposing circle to port with input ±90

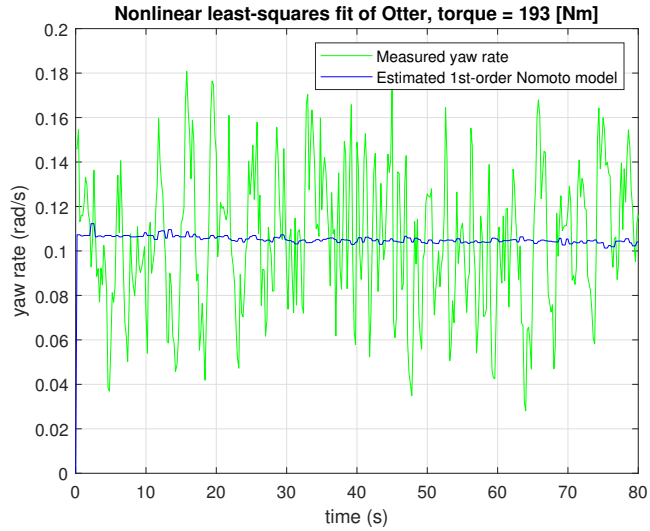

(b) Opposing circle to starboard with input ±90

Figure 4.3

Opposing circle (±90)		
	Model parameters (Port)	Model parameters (Starboard)
K	$7.6554 \cdot 10^{-4}$	$5.5886 \cdot 10^{-4}$
T	0.8657	0.0113

Table 4.4: Identified model parameters for fast opposing circle

Slow Turning

In figure 4.4b and 4.5b the measured yaw rate tends to oscillate, this can be due to small waves. The USV's turning ability is more affected by waves at lower speed.

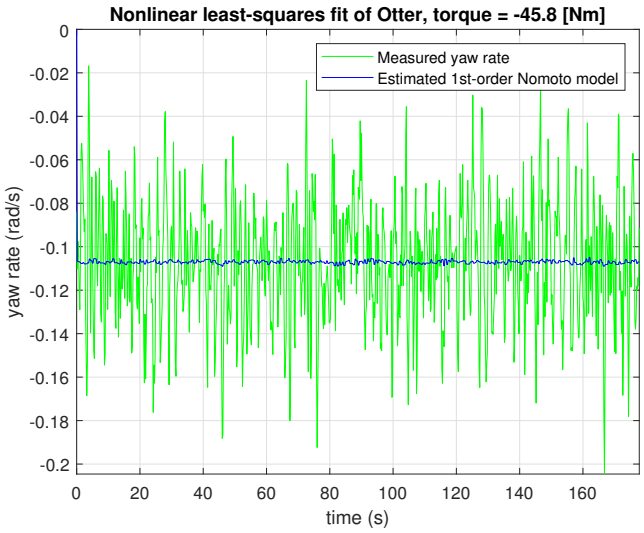

(a) Slow opposing circle to port with input ±40

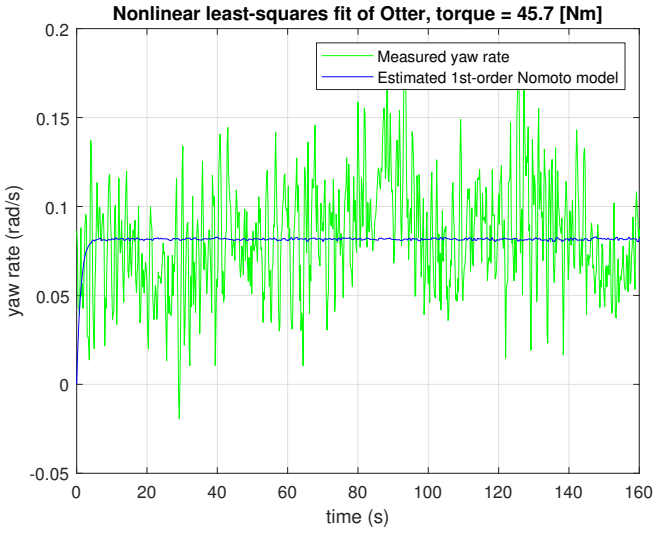

(b) Slow opposing circle to starboard with input ±40

Figure 4.4

Opposing circle (±40)		
	Model parameters (Port)	Model parameters (Starboard)
K	0.0023	0.0018
T	0.0127	1.1161

Table 4.5: Identified model parameters for slow opposing circle

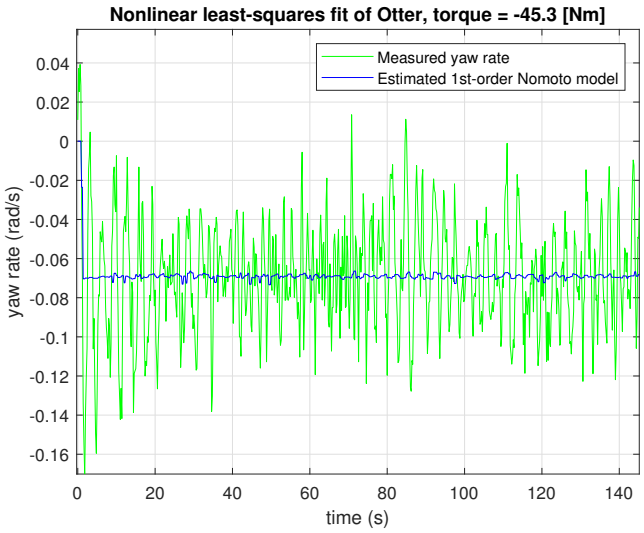

(a) Slow additive circle to port with input 60/15

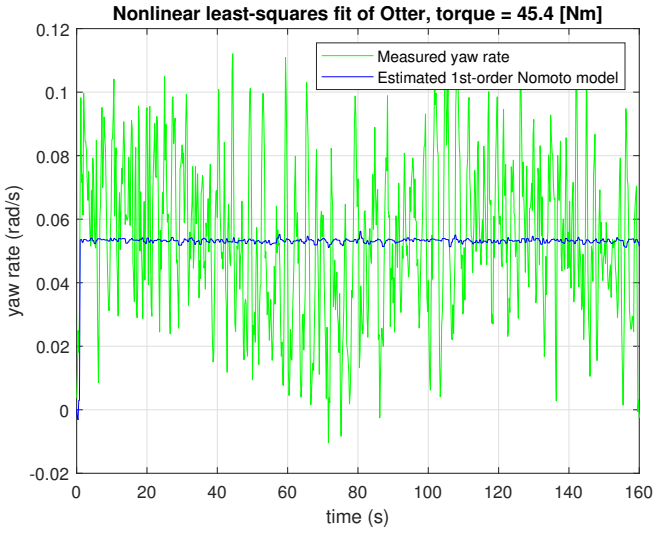

(b) Slow additive circle to starboard with input 60/15

Figure 4.5

Additive circle (60/15)		
	Model parameters (Port)	Model parameters (Starboard)
K	0.0015	0.0012
T	0.7591	0.392

Table 4.6: Identified model parameters for slow additive circle

4.3 Simulated Models

After I obtained the identified parameters from the turning circle tests, I built a small simulator in Simulink. The purpose of the simulator is to compare the following proposed Nomoto models with different torque inputs to compare the precision of the model.

4.3.1 Proposed Nomoto Model Without Correction Terms

The proposed model for fast turning is

$$\frac{r}{u_1} = \frac{K}{Ts+1} \tag{4.1}$$

were $K = 0.0008$ and $T = 0.5$. The Nomoto gain was found by taking the average of all the estimated Nomoto gains, K, displayed in table 4.3 and 4.4. In figure 4.6 the red line is the proposed model's response to an input when the Otter USV is performing an additive circle with 100% on one thruster and 25% on the other one, depending on which way the USV is turning.

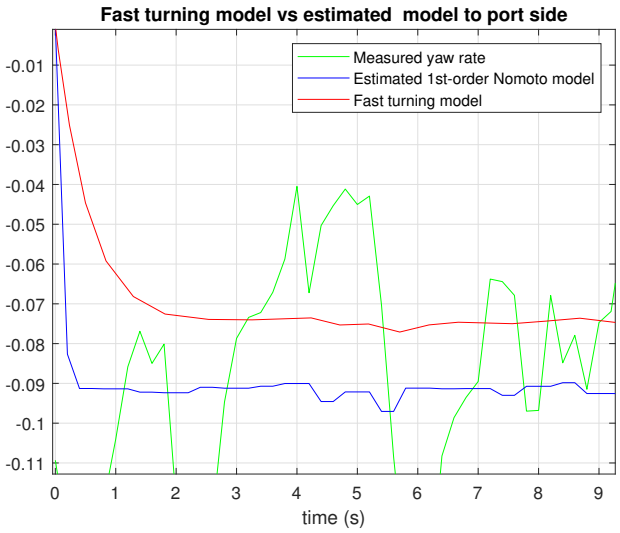

(a) Fast model with input from additive circle 100/25 to port

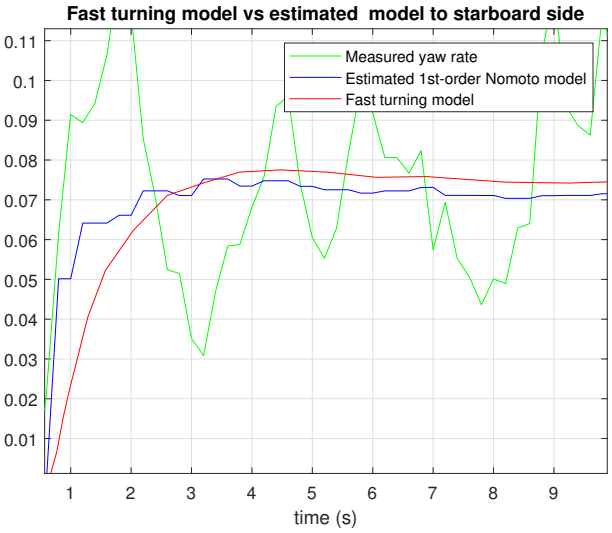

(b) Fast model with input from additive circle 100/25 to starboard

Figure 4.6

The response to starboard side is much more precise than to port side, as depicted in figure 4.6.

The proposed model for slow turning is

$$\frac{r}{u_1} = \frac{K}{Ts+1} \tag{4.2}$$

were $K = 0.0017$ and $T = 0.7$. The Nomoto gain was found by taking the average of all the estimated Nomoto gains, K, displayed in table 4.6 and 4.5. The input to the model

is when the Otter USV are performing an opposing circle with 40% of maximum throttle.

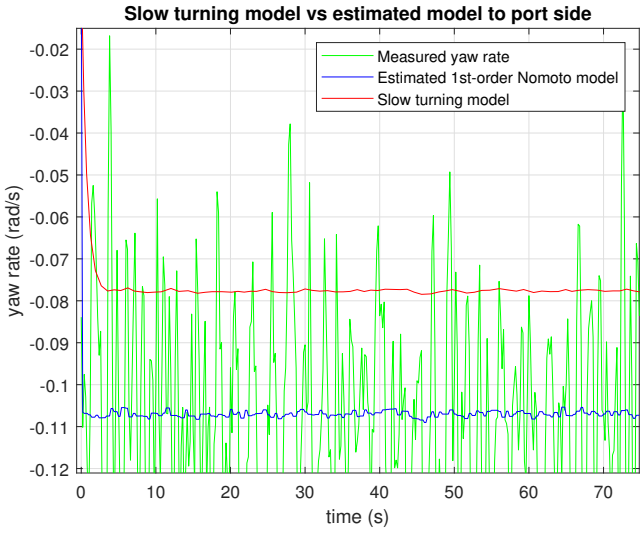

(a) Response of the slow model to port side

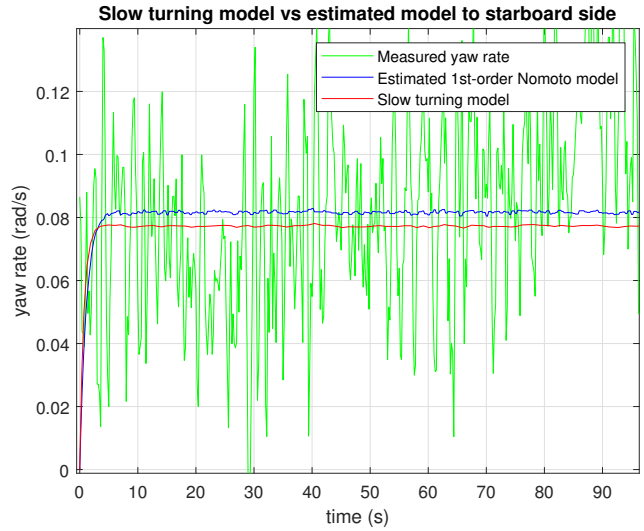

(b) Response of the slow model to starboard side

Figure 4.7

4.3.2 Proposed Nomoto Model With Correction Terms

The models proposed in the last section do not take into account the extra torque to port side produced due to the propellers rotating in the same direction when moving forward.

By introducing two correction terms to the torque input, the idea is to remove the offset to port side. The correction terms depend on the thrust from each propellers.

$$T\dot{r} + r = K \underbrace{(\mathbf{F}_{port} - \mathbf{F}_{starboard})a}_{T_p} - \rho \mathbf{F}_{port} - \sigma \mathbf{F}_{starboard} \tag{4.3}$$

where ρ and σ are tuning parameters. The tuning parameters were chosen to be $\rho = \frac{0.00002}{K}$ and $\sigma = \frac{0.00008}{K}$. The tuning parameters were tuned with respect to the same K as was found in section 4.3.1.

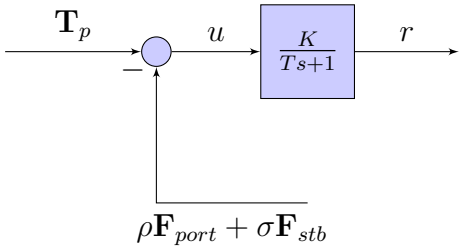

Figure 4.8: Block diagram of input with correction terms

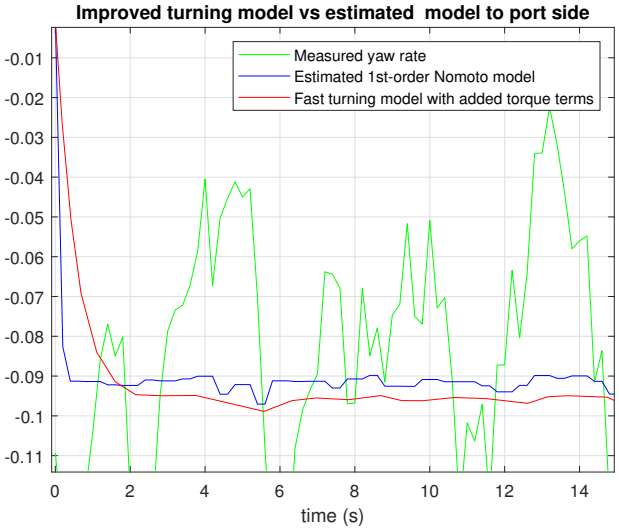

(a) Additive circle to port

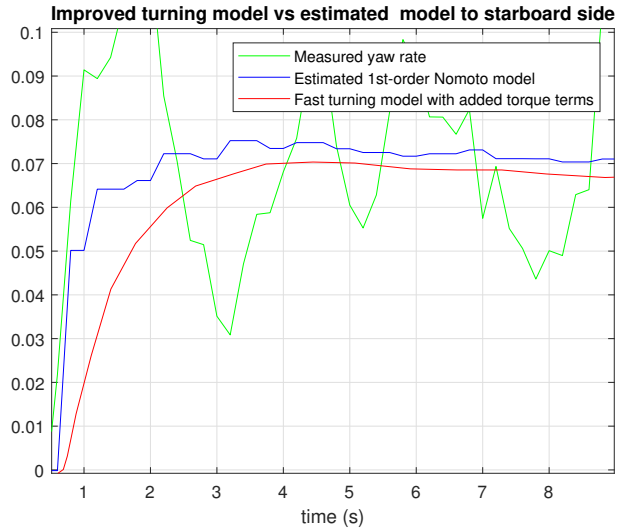

(b) Additive circle to starboard

Figure 4.9

Figure 4.6 and 4.9 the correction terms manage to compensate for the extra torque to port side, due to the propellers rotating the same way. However, for the opposing ±90 turning circle the correction terms does not yield any correction. When the speed is large and the thrusters are opposing the relationship between the input torque and the yaw rate seems to have a nonlinear relationship, and consequently, the linear model does not manage to give a good correction. This is depicted in figure 4.10

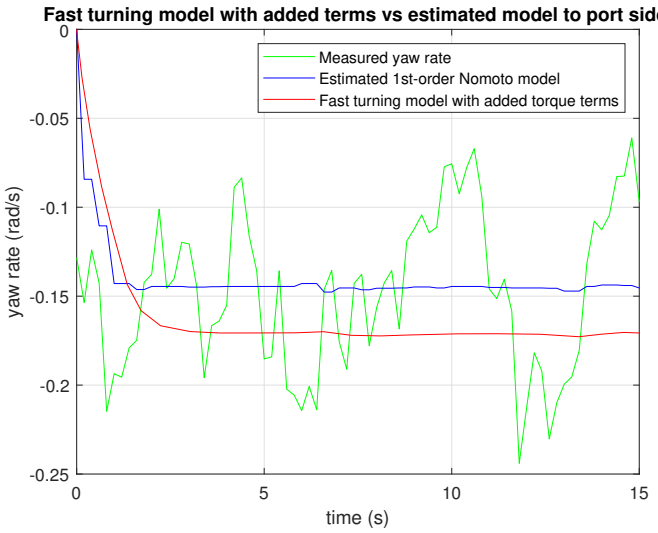

(a) ±90 opposing circle to port

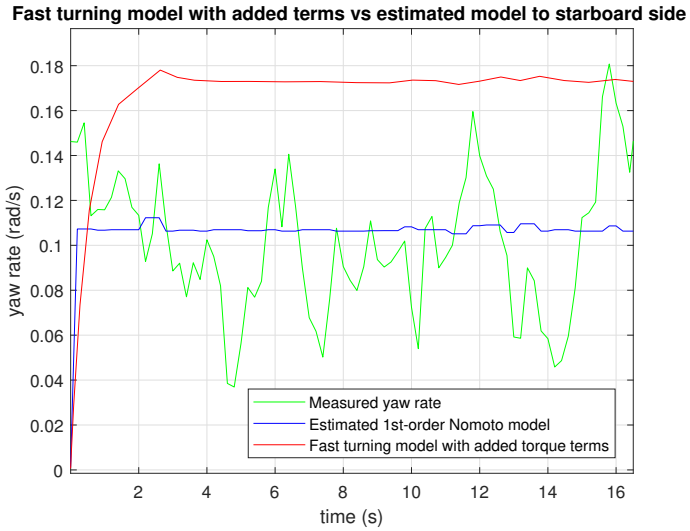

(b) ±90 opposing circle to starboard

Figure 4.10

A Nomoto model with correction terms was not performed for the slow turning data. This is due to the waves experienced at the test site, meaning that the data obtained is not suitable for the model in the first place. I see therefore no point to attempt making a better model before the tests are redone.

4.4 Discussion

In this thesis I have described the system identification of the Nomoto model using turning circle tests. First, I gathered experimental data from a bollard pull test to obtain a square thruster model. Then a thrust allocation was made for the Otter USV which was used as an input in the Nomoto model. The experimental data from the turning circles were used to calculate model parameters for all turning circle tests, using a nonlinear curve fitting method. Unfortunately, a zigzag test was not executed due no access to the compass during the tests. The zigzag test would have contributed with valuable information about the dynamics of the USV, but also to the Nomoto gain, K. However, two models were made. One for fast turning and one for slow turning.

The models can be used in a model based controller, where they can generate feed-forward and feedback signals which can be used in a control system for the Otter USV.

4.4.1 Discovery of Additional Torque

Though I have made an approximate model to a specific question, there are clear limitations to the test and the model. There are however some interesting discoveries that were done testing and modelling the USV. During tests, I discovered that when the USV is turning towards port side, it has an offset compared to starboard side. This is likely due to the propellers of the Otter USV which are both rotating in clockwise rotation when moving forward, and anti-clockwise when moving backwards. When both propellers move in the same direction the USV can be lurching due to conservation of angular momentum. This could indeed explain the asymmetry to port and starboard.

4.4.2 Noise and Disturbances

During live testing, I performed acceleration tests for different forward speeds. The yaw rate measured during these tests could have been used to estimate the standard deviation of the yaw rate, to explore if this rates depends on the speed. These results could then have been used to estimate the noisiness of the IMU. However, when the acceleration test were performed the logging of the yaw rate was not working, so I could not measure the yaw rate.

A different observation is that the propellers do not manage to rotate with constant velocity and have small oscillations around a mean value which varies with maximum 4%. This could be due to the propellers being interrupted by water flow, but measurement errors from the tachometer can also contribute. I did not observe any consistent error in

these oscillations when the Otter USV was turning to port or starboard side. However, all measurements are done only once, which infers uncertainty around the reproducibility of the measurements.

When performing a turning circle for this test's purpose, environmental disturbances should not be present. Certain environmental conditions such as waves and currents are forces that affects the test. When we performed the tests in November, some waves and most likely current were present, which most likely have contributed to inaccuracies in the measurements.

4.4.3 Thruster Efficiency

Another discovery is the lack of efficiency when the Otter USV performs a fast opposing circle. Comparison between figure 4.2 and 4.3, tells that the input torque for the opposing circle is the double of the additive circle. This could be explained by the propellers are less effective when rotating backwards, due to asymmetry in the propeller design. Another smaller effect can be if the thrusters are depending on the advance speed, reducing the general control force with increasing advance speed. If the bollard pull test was performed with different advance speed, the propulsion model generated by the data from the bollard pull test (2.9) could have yielded a more accurate model for the propellers. Unfortunately, this was not done due to no access to a towing tank.

Another limitation to the tests performed with the USV, arises when the throttle is over 80%, where the propellers seem to have reached maximum rpm, which is depicted in figure 4.1.

4.4.4 Proposed Models

It is evident that the slow model is more inaccurate compared to the fast model, which is most likely because of the waves which colluded with the measurements in the slow turning tests.

The proposed Nomoto model with correction terms for the input torque manage to add the additional torque which is present due to the propellers rotating in the same direction. It also manage to compensate when turning to starboard side. The exception is for the opposing ± 90 circle. This can be explained by a nonlinear relation between the input torque and the yaw rate due to large speed and opposing thrusters

If I was to perform these tests again, I would have focused on performing the same tests several times. I would also consider to perform the tests inside, in a more controlled

environment. A zigzag test could tell more about the dynamics of the Otter USV, and is another way of calculating the parameters and can be used to compare the results for the different model parameters.

Chapter 5

Conclusion

The overall goal of the project was to make an autopilot model for the Otter USV and identify the model parameters using system identification. In this report I have live tested and determined system parameters for the Nomoto model, as well as computed the general control forces from the thrust allocation from the fixed propellers. Based on the obtained simulation results with correction terms on the input, the model manages to obtain an accurate result compared with actual measurements. This indicates that the model is fairly accurate, and the Nomoto model is a good fit. The reliability of the model parameters starts with the data it is based on. In this case, the manoeuvring tests were not performed under optimal conditions, so that the data obtained is contributing to uncertainties in the model. Despite that, the Nomoto model with correction terms manages to describe the heading dynamics for the Otter USV. It is however difficult to know how much model insecurity is accepted before it is used in its intended area.

In short, this report describes that the Nomoto model is a good fit as a system model for the Otter USV, when the Otter USV is performing fast turning and the correction terms are accounted for in the model.

5.1 Recommendations for Further Work

The major problems encountered when making this model is the data. I believe that redo all the experimental tests under optimal conditions would contribute to making a more accurate model. As the weather in Trondheim is always uncertain, I would highly suggest that all tests were performed indoors in a tank to minimise disturbances. In future experiments, the bollard pull test should also be performed with advance speed, which would give a more accurate thruster model. This can be done in a towing tank. Furthermore, the turning circles should be redone for slow turning, in order to obtain data

which is not overly influenced by environmental disturbances. If possible, a zigzag test should be preformed to obtain more information about the dynamics. Further on, these models (for fast and slow turning) can be used in a model based controller to generate feed forward and feedback signals, which can be used to control the Otter USV.

Bibliography

Azarsina, F. and Williams, C. D. (2012). Nomoto indices for constant-depth zigzag manoeuvres of an autonomous underwater vehicle. *ISRN Oceanography*.

Blanke, M., Pivano, L., and Johansen, T. A. (2007). An efficency optimizing propeller speed control for ships in moderate seas - model experiments and simulations. *IFAC Proceedings Volumes*, 40:329–336.

Breivik, M. (2010). *Topics in Guided Motion Control of Marine Vehicles*. PhD thesis, Norwegian University of Science and Technology, Faculty of Information Technology, Mathematics and Electrical Engineering Department of Engineering Cybernetics.

Fossen, T. (2011). *Handbook of Marine Craft Hydrodynamics and Motion Control*. John Wiley & Sons.

Gertler, M. and Gover, S. C. (1960). Handling criteria for surface ships. Technical report dtmb-1461, Naval Ship Research and Development Center, Washington D.C.

Golikov, V. A., Golikov, V. V., Volyanskaya, Y., Mazur, O., and Onishchenko, O. (2018). A simple technique for identifying vessel model parameters. *IOP Conference Series: Earh and Environmental Science*.

ITTC (2002). ITTC – Recommended Procedures. *ITTC _ Recommended Procedures*.

Journée, J. (1970). A simple method for determining the manoeuvring indices k and t from zigzag trial data. Technical report, Delft University of Technology.

Jukola, H. and Skogman, A. (2002). Bollard pull. *Proceedings of the 17th International Tug and Salvage Convention, ITS*.

Kartverket (2018). Vannstands- og tidevannsinformasjon trondheim. https://www.kartverket.no/sehavniva/sehavniva-lokasjonside/?cityid=9000021&city=Trondheim. Accessed: 2018-11-28.

Li, Z. and Bachmayer, R. (2013). The development of a robust Autonomous Surface Craft for deployment in harsh ocean environment. *2013 OCEANS - San Diego*, pages 1–7.

Ljung, L. (1998). *System Identification: Theory for the User*. Prentice Hall.

Mathworks (2018). Solve nonlinear curve-fitting (data-fitting) problems in least-squares sense - lsqcurvefit. https://se.mathworks.com/help/optim/ug/lsqcurvefit.html. Accessed: 2018-12-06.

Moreira, L., Fossen, T. I., and Soares, C. G. (2005). Modeling, guidance and control of "Esso Osaka" model. In *IFAC Proceedings Volumes (IFAC-PapersOnline)*.

Nomoto, K. (1960). Analysis of kempf's starndard maneuver test and proposed steering quality indices. *First Symposium on Ship Maneuverability*, Report 1461:275–304.

Nomoto, K., Taguchi, T., Honda, K., and Hirano, S. (1957). On the steering qualities of ships. *International Shipbuilding Progress*, 4:354–370.

.1 Bollard Pull Test

.1.1 thruster_parameters.m

```
close all
clear all
clc


T_rotation = [0 122.4 243.7 358.8 490.5 615.8 725.6 844.6 981.4 980.6 980.9]'*pi/30; % mean of both thrusters
Force = [0 0.8 1.3 2.9 5.4 8.7 12.2 17.7 23.3 23.1 23.7]'*9.81;

%% Nonlinear Least Squares

% Model: ax^2+bx
s = fitoptions('Method','NonlinearLeastSquares',...
               'Lower',[0,0],...
               'Upper',[inf,max(T_rotation)],...
               'Startpoint',[0 0]);

f1 = fittype('a*x^n+b*x','problem','n','options',s);

[nlsq,gof] = fit(T_rotation,Force,f1,'problem',2);


figure(3)
plot(nlsq)
hold on
scatter(T_rotation, Force)
xlabel("\omega [rad/s]")
ylabel("Thrust [N]")



title("Model: t_{nn}*|x|x + t_{nu}*|x|u_a")
hold off


legend('line fit', 'measured data')

% Model: ax^2
s2 = fitoptions('Method','NonlinearLeastSquares',...
               'Lower',[0,0],...
               'Upper',[inf,max(T_rotation)],...
               'Startpoint',[0]);

f2 = fittype('a*x^n','problem','n','options',s2);

[nlsq2,gof2] = fit(T_rotation,Force,f2,'problem',2);


figure(4)
plot(nlsq2)
hold on
scatter(T_rotation, Force)
xlabel("\omega [rad/s]")
ylabel("Thrust [N]")
```

```
54
55
56 title("Model: k*|x|x")
57 hold off
```

.1.2 bollard_pull_test.m

```
1  clear all
2  close all
3  clc
4
5  % Extract RPM data from file
6  load bollard_data.csv;
7
8  %% 10% thrust
9  stb_10 = bollard_data(10159:10192,12);
10 port_10 = bollard_data(10159:10192,13);
11 stb_10_mean = mean(stb_10);
12 port_10_mean = mean(port_10);
13
14 meas_10 = (stb_10_mean+port_10_mean)/2;
15
16 %% 20% thrust
17 stb_20 = bollard_data(10484:10541,12);
18 port_20 = bollard_data(10484:10541,13);
19 stb_20_mean = mean(stb_20);
20 port_20_mean = mean(port_20);
21
22 meas_20 = (stb_20_mean+port_20_mean)/2;
23
24
25
26 %% 30% thrust
27 stb_30 = bollard_data(10581:10615,12);
28 port_30 = bollard_data(10581:10615,13);
29 stb_30_mean = mean(stb_30);
30 port_30_mean = mean(port_30);
31
32 meas_30 = (stb_30_mean+port_30_mean)/2;
33
34
35 %% 40% thrust
36 stb_40 = bollard_data(10813:10831,12);
37 port_40 = bollard_data(10813:10831,13);
38 stb_40_mean = mean(stb_40);
39 port_40_mean = mean(port_40);
40
41 meas_40 = (stb_40_mean+port_40_mean)/2;
42
43
44 %% 50% thrust
45 stb_50 = bollard_data(10998:11056,12);
46 port_50 = bollard_data(10998:11056,13);
47 stb_50_mean = mean(stb_50);
48 port_50_mean = mean(port_50);
49
50 meas_50 = (stb_50_mean+port_50_mean)/2;
```

```
51
52 %% 60% thrust
53 stb_60 = bollard_data(11129:11186,12);
54 port_60 = bollard_data(11129:11186,13);
55 stb_60_mean = mean(stb_60);
56 port_60_mean = mean(port_60);
57
58 meas_60 = (stb_60_mean+port_60_mean)/2;
59
60
61 %% 70% thrust
62 stb_70 = bollard_data(11219:11277,12);
63 port_70 = bollard_data(11219:11277,13);
64 stb_70_mean = mean(stb_70);
65 port_70_mean = mean(port_70);
66
67 meas_70 = (stb_70_mean+port_70_mean)/2;
68
69
70 %% 80% thrust
71 stb_80 = bollard_data(11369:11426,12);
72 port_80 = bollard_data(11369:11426,13);
73 stb_80_mean = mean(stb_80);
74 port_80_mean = mean(port_80);
75
76 meas_80 = (stb_80_mean+port_80_mean)/2;
77
78
79
80 %% 90% thrust
81 stb_90 = bollard_data(11603:11654,12);
82 port_90 = bollard_data(11603:11654,13);
83 stb_90_mean = mean(stb_90);
84 port_90_mean = mean(port_90);
85
86 meas_90 = (stb_90_mean+port_90_mean)/2;
87
88
89
90 %% 100% thrust
91 stb_100 = bollard_data(11900:11917,12);
92 port_100 = bollard_data(11900:11917,13);
93 stb_100_mean = mean(stb_100);
94 port_100_mean = mean(port_100);
95
96 meas_100 = (stb_100_mean+port_100_mean)/2;
```

.2 Parameter Identification

```
1 clear all
2
3 %%%%%%%%%%%%%%%%%%%%%%%% TURN PORT +-90 %%%%%%%%%%%%%%%%%%%%%%%%%%%%%%%%
4 %%%%%%% thr_port = -0.9
5 %%%%%%% thr_starboard = 0.9
6 %%%%%%% rpm_port = 1002
7 %%%%%%% rpm_stb = 990
```

```
%%
load data.csv
starting = 58777;                       %Start point for the test
ending = 59640;                         %Endpoint for the test

yaw_rate = data(starting:ending,7);
thr_stb = data(starting:ending,12);
thr_port = -data(starting:ending,13);

k = 0.0002373;                          %Thruster parameter [rpm]
F_stb = k.*thr_stb.*abs(thr_stb);       %Thrust from starboard thruster
F_port = k.*thr_port.*abs(thr_port);    %Thrust from port thruster
a = 0.395;                              %Moment arm
M = (F_port-F_stb)*a;                   %Input torque



%% unfiltered +- 90
y = yaw_rate;
N = ending-starting+1; % samples
f = 5; % Hz
time = (0:0.2:((N-1)/f))';

x0 = [0.1  1]';

F = @(x,time)(exp(-time*x(1))*0 + x(2)*(1-exp(-time*x(1))).*M);
x = lsqcurvefit(F,x0, time, y);

T = 1/x(1)
K = x(2)

figure(2)
plot(time,y,'g',time,exp(-time*x(1))*0 + x(2)*(1-exp(-time*x(1))).*M,'b'),grid
title('Nonlinear least-squares fit of Otter, torque = -186 [Nm]'),xlabel('time (s)'),
    ylabel('yaw rate (rad/s)')
legend('Measured yaw rate','Estimated 1st-order Nomoto model')
xlim([0  178.6])
```

.3 Simulation

```
%%
load data.csv;

%% Input to simulation
starting = 58777;
ending = 59640;
yaw_rate = data(starting:ending,7);
thr_stb = data(starting:ending,12);
thr_port = -data(starting:ending,13);

k = 0.0002373;                  % N/rpm^2
F_stb = k.*thr_stb.*abs(thr_stb);
F_port = k.*thr_port.*abs(thr_port);
a = 0.395;
M = (F_port-F_stb)*a;

```

```
N = ending-starting+1;                  % samples
f = 5;                                  % Hz
time = (0:0.2:((N-1)/f))';

% Model parameters
K = 0.0008;
T = 0.5;

% Correction terms
si_p = sign(mean(thr_port));
si_s = sign(mean(thr_stb));
p = 0.00002/K*si_p;                     %Correction parameter port
s = 0.00008/K*si_s;                     %Correction parameter starboard

C = p*abs(F_port) + s*abs(F_stb);

torque =timeseries(M,time);             %Input torque
corr = timeseries(C,time);              %Calculated correction



%% simulate model

sim model_sim

%% plot simulated output in original
hold on
plot(tout,yaw_rate_sim,'r')
hold off
```

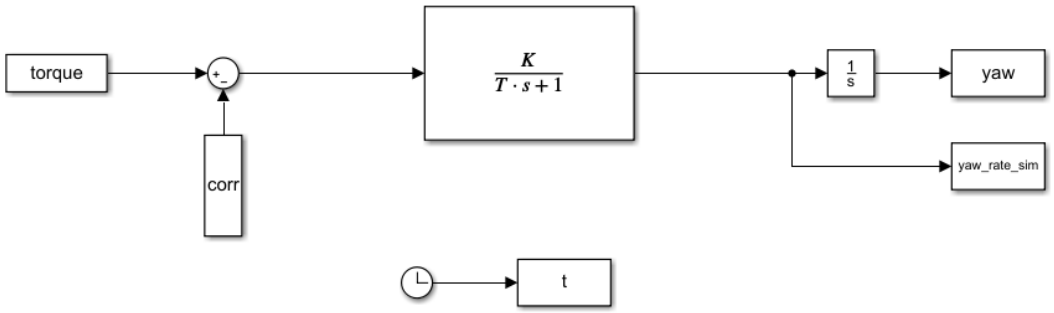

Figure 1: Structure of the simulator